Desalination and Water Treatment
www.deswater.com
doi: 10.5004/dwt.2021.27041

221 (2021) 185–196
May

Synthesis and characterization of activated carbon from *Capparis decidua* for removal of Pb(II) from model aqueous solution: kinetic and thermodynamics approach

Muhammad Bilal[a,*], Javed Ali[a], Muhammad Yaseen Khan[a], Rafi Uddin[a], Farina Kanwl[b]

[a]*Department of Chemistry, Kohat University of Science and Technology, Kohat KPK, Pakistan, emails: bilalhej@gmail.com (M. Bilal), javedgm@gmail.com (J. Ali), yaseenkust365@gmail.com (M. Yaseen Khan), rafibangash002@gmail.com (R. Uddin)*
[b]*Pakistan Council of Scientific and Industrial Research Labs Complex, Peshawar, Pakistan, email: farinakanwal@gmail.com*

Received 19 March 2020; Accepted 15 January 2021

ABSTRACT

Eco-friendly biomass and its activated carbon synthesized from the stem of *Capparis decidua* was attempted for removal of Pb(II) from model aqueous solution. Raw biomass and its activated carbon composition were analyzed by thermogravimetric analysis, scanning electron microscopy, energy-dispersive X-ray analysis and Fourier-transform infrared analysis. Various parameters such as, concentration of the metal ion, contact time, temperature, particle size of the adsorbent, pH, dosage of adsorbent and influence of shaking speed in batch experiments were investigated. Pb(II) removal from aqueous solution obeyed pseudo-second-order kinetics equation having a good correlation coefficient value of (R^2 = 0.9995 and 0.9995). Freundlich isotherm model was well fitted and adsorption capacity (q_m) was found 327.86 mg/g for biomass and 719.42 mg/g on activated carbon. The adsorption of Pb(II) was increased with an increase of pH on both the raw biomass and activated carbon. The pH value for point of zero charge on activated carbon was found 8.8. Thermodynamics parameter, that is, $\Delta G°$, $\Delta H°$ and $\Delta S°$ were also calculated which clued that process of Pb(II) adsorption on biosorbents was spontaneous and exothermic. The interaction of Pb(II) with adsorbent was physical in nature.

Keywords: Pb(II) removal; Adsorption model; Thermodynamics study; Wastewater treatment; Activated carbon from *Capparis decidua*

1. Introduction

Different effluents coming from industries such as mining, electroplating, electrolysis, leather, electro-osmosis, fertilizer, photography, mining, smelting, battery preparation industry, petroleum refining, paint, pesticides are the main source of Pb(II) in water [1,2]. Pb(II) is one of the toxic metals which may cause anorexia, intestinal problem, mental issues in children, anaemia, brain impairment, loss of appetite, liver cirrhosis and Fanconi syndrome in kidneys [3,4]. To defend public health from heavy metal ions, its removal from industrial effluents is important [2]. Different biological, biochemical, and physiochemical processes have been attempted for removal of these hazardous metals from contaminated water. In these methods include, electrochemical analysis (electrocoagulation, electroflotation, and electrodeposition), physicochemical operations, biosorption (ACs, CNTs, and adsorbents from plant and livestock), or modern techniques (membrane filtration methods, catalysis, and nanotechnology) [5]. Adsorption is one of the most preferred and effective methods used for removing of the lethal metal from waste water due to its simple design, easy operation, and relatively simple regeneration and cost beneficial. Different agricultural by-products and waste were investigated for preparation of green adsorbent. Among these include shells

* Corresponding author.

of almond [6], stones of apricot [7], saw dust [8], rice hulls and husks [9], *Oryza sativa* husk [10], shells of coconut fruit [11], bark of eucalyptus [12], orange peel [13], peach stones [14], sugarcane bagasse [15], white dragon fruit [16], rock melon [17], bitter gourd [18]. Although, these methods are used successfully for the adsorption processes [19], search for biosorbent having high sorption capacity and low cost are still main target of environmental chemists.

Among the various renewable available resources, use of *Capparis decidua* stem as raw materials for activated carbon is a new source for biosorbent which are not investigated before for removal of Pb(II). It is a member of family Capparaceae and has a bushy shrub with a height of 4–5 m. This plant is easily available in tropical region of the world, that is, sub-continent (India and Pakistan) and Africa which is currently used only for combustion purpose. The utilization of *Capparis decidua* stem for the production of AC may minimize the pollution problems and considered as low-cost precursor for preparation of AC. The current study was therefore based on adsorption of Pb(II) from model waste water solution on raw biomass and its ACs using *Capparis decidua* stem.

2. Experimental

2.1. Chemicals

All the given chemicals were analytical grade and was used as such received from the company. Hydrochloric acid (37%), nitric acid (69%) was purchased from Riedel-de Haen Sigma-Aldrich. Sodium hydroxide (98%), lead acetate trihydrate (99.99%) was supplied by MERCK, KGaA, Darmstadt, Germany.

2.2. Raw biomass and its activated carbon

Capparis decidua stem were collected from Jarma Graveyard, near Kohat University of Science and Technology, Kohat-26000, Khyber Pakhtunkhwa, Pakistan, washed several time with distilled water in order to clean the sample and dried in open air for few days. Activated carbon (ACs) was prepared by using powder form of the stem of the given plant in furnace (Tetec XTMA series temp cont.) at 600°C for 60 min and were sieved through sieve (ASTM E11, Gilson's Company, USA) in Kohat Cement Factory, Pakistan to obtain particle size (90–250 μm).

2.3. Characterization of biomass and its ACs

For thermogravimetric analysis (TGA) (Pyris Diamond Series, Perkin Almer, USA) was used. The sample was thermally treated in an inert atmosphere (N_2) from room temperature to 1,000°C with a ramp of 10°C/min. The presences of different functionalities present in samples were analyzed by using Fourier-transform infrared (FTIR) spectrometer (Spectrum two, Perkin Almer, USA). Each sample was analyed by the KBr method in the range of 4,000–400 cm^{-1}. Surface topography was analyzed using scanning electron microscopy (SEM) (JSM5910 JEOL, Japan). The sample was characterized without any gold plating. Tungsten filament was used for electron beam production. The chemical characterization was analyzed using energy-dispersive X-ray spectrometer (EDS) (INCA200/Oxford instruments, UK).

2.4. Adsorption study

Batch experiment mode was used for checking the adsorption capacity of the biosorbent. In each analysis, known concentration of Pb(II) solution was added in 100 mL flask. The mixture of biosorbent and Pb(II) solution was agitated on a shaker (Wise Bath, WSB-30, DIAHAN Scientific Co., Ltd., Seoul, Korea) with ramp of 140 cycle/min and at desired temperature. Sufficient time was allowed for adsorption equilibrium. Shaking speed allows surface of biosorbent to come in contact with metal ion in these experiments. Different parameters i.e. contact time, amount of biosorbent, metal ion concentration, pH, speed of shaking (rpm), temperature and size of biosorbent particle were examined for adsorption of Pb(II) on biomass and ACs of *Capparis decidua* stem. After experiment, Pb(II) concentration in filtrates were analyzed on atomic absorption spectrometer (A Analyst 400, Perkin Elmer, USA).

The capacity of metal ion removal efficiency on biosorption are defined as [20]:

$$\text{Adsorption capacity, } q_e = \frac{\{C_i - C_v\}V}{m} \quad (1)$$

$$\%\ \text{Adsorption of Pb(II)} = \frac{\{C_i - C_e\}}{C_i} \times 100 \quad (2)$$

where q_e is the adsorbed amount of metal at equilibrium in mg/g; C_i and C_e are initial and equilibrium concentration (mg/L), m is the amount of the adsorbent (g) and V is the volume of the solution (L).

2.5. Point of zero charge

Point of zero charge value for the adsorbents were determined by salt addition technique [21]. In different flask, 0.1 M sodium nitrate (40 mL) and 0.1 g adsorbent were added. pH_1 (2, 4, 6, 8, 10, 12) was adjusted using either 0.1 M nitric acid or 0.1 M sodium hydroxide solutions. All the bottles were agitated on shaker for 24 h at 25°C. Final pH_2 reading was carefully noted and ΔpH (pH_2–pH_1) was determined. The initial pH values were plotted against ΔpH results. The intersection of the connecting point line with the horizontal axis at the point ΔpH = 0 indicates pH_{PZC}. This process was repeated for biomass and ACs of *Capparis decidua* stem.

2.6. Adsorption kinetics

For kinetic study, 0.1 g of biosorbent and 50 mL Pb(II) solution was poured to 250 mg/L flask and agitated with ramp of 140 cycle/min at 25°C. Under the given conditions the adsorption experiment was performed for different interval of time (from 5 min to 180 min) separately. Then pseudo-first-order and pseudo-second-order kinetics equation were applied to calculate the kinetic data for removal of Pb(II) using biomass and activated carbon as a adsorbents.

The equation used for pseudo-first-order kinetics is given below [22]:

$$\log\left\{q_e - q_t\right\} = \log q_e - \left(\frac{k_1}{2.303}\right)t \tag{3}$$

While for pseudo-second-order kinetics following equation was tried [23]:

$$\frac{t}{q_t} = \frac{1}{k_2 q_e^2} + \frac{t}{q_e} \tag{4}$$

where q_e and q_t represent the adsorbed amount of Pb(II) at equilibrium time and time (t) in (mg/g). k_1 represent the rate constants for pseudo-first-order and k_2 represent the rate constants for pseudo-second-order kinetics. The values of q_e, k_1 and k_2 were calculated from the equations.

2.7. Adsorption isotherm

Biosorbent and activated carbon (0.1 g) were added in 50 mL Pb(II) solution and agitated with ramp of 140 cycle/min for 60 min. Using the mentioned condition, adsorption of different initial metal concentration upto 1,000 mg/L were tested separately. Then two well-known adsorption isotherms, that is, Langmuir and Freundlich isotherm models were used to study adsorption results. Langmuir model considers monolayer adsorption of the adsorbate on the homogeneous surface of the adsorbent [24,25] equation:

$$\frac{C_e}{q_e} = \frac{1}{q_m K_L} + \frac{C_e}{q_m} \tag{5}$$

where C_e is a concentration of Pb(II) ions (mg/L) at equilibrium, q_e is the amount of adsorbed Pb(II) calculated at equilibrium (mg/g), K_L is the constant for Langmuir isotherm, q_m illustrates the maximum capacity of Pb(II) adsorption.

The heterogeneity of the surface of biosorbent and ACs favors multilayer formation. Kenneth R. Hall in 1966 introduces a separation factor R_L a dimensionless equilibrium term, to express the Langmuir constant K_L. The importance of the R_L term is based upon an initial assumption of the applicability of the obtained results of the Langmuir isotherm model, beyond which the value of R_L provides important information about the adsorption isotherm. The separation factor equation can be determined by the equation [26]:

$$R_L = \frac{1}{1 + R_L C_0} \tag{6}$$

where K_L is the constant of Langmuir isotherm equation, C_0 is initial concentration of adsorbate (mg/L). The value of R_L represents the type of isotherm to be either favorable ($0 < R_L < 1$), unfavorable ($R_L > 1$), or irreversible ($R_L = 0$).

Freundlich isotherm well explain the interaction between adsorbent and adsorbate on the surface of heterogeneous adsorbent.

The below equation was applied to evaluate the Freundlich isotherm model [25]:

$$\log q_e = \log K_f + \frac{1}{n}\log C_e \tag{7}$$

where K_f represent Freundlich constant which represents relative adsorption capacity of adsorbent (mg/g) $(dm^3/mg)^{1/n}$, $1/n$ is Freundlich represent the intensity of adsorption, while q_e is the amount adsorbed (mg/g) of the adsorbate at equilibrium, and C_e is the equilibrium concentration (mg/L).

2.8. Adsorption thermodynamics

Thermodynamic parameters, that is, change in Gibbs free energy, enthalpy and entropy were calculated with the help of thermodynamic equilibrium constant K_0 at different temperature [26]. From the results of $\Delta G°$ calculated the feasibility of the Pb(II) adsorption on biosorbents.

The value of K_0, $\Delta G°$ and $\Delta H°$ can be calculated using the equations below:

$$K_0 = \frac{a_s}{a_e} = \frac{v_s}{v_e}\frac{C_s}{C_e} \tag{8}$$

$$\Delta G° = -RT\ln K° \tag{9}$$

$$\ln K°\left(T_2\right) - \ln K°\left(T_1\right) = \frac{-\Delta H°}{R}\left(\frac{1}{T_2} - \frac{1}{T_1}\right) \tag{10}$$

$$\Delta S° = -\frac{\Delta G° - \Delta H°}{T} \tag{11}$$

where, a_s represents the activity of Pb(II)ion, a_e shows the activity of Pb(II) ion in solution at equilibrium, C_s represents the amount of Pb(II) adsorbed per gram of adsorbent (mmol/g) and C_e shows at equilibrium the Pb(II) concentration in solution (mmol/ml), V_s is the activity coefficient of adsorbed Pb(II) and V_e is the activity coefficient of Pb(II) in solution. As the concentration of Pb(II) in solution decreases and access to zero, the value of $K°$ were calculated by plotting $\ln(C_s/C_e)$ vs. C_s and considers the C_s to be zero. The straight line obtained and from the intercept on y-axis calculate the values of $K°$. R is the general gas constant and T is the temperature. The average value of $\Delta H°$ can be determined from van't Hoff equation. T_2 (278 K) and T_1 (273 K) represent the final and initial temperature.

3. Results and discussion

3.1. Characterization of raw biomass and ACs

TGA analysis is primarily applied to investigate the thermal or oxidative stability of biosorbent as well as their compositional properties [27]. TGA was conducted in inert atmosphere from 25°C to 1,000°C with the heating rate of 10°C/min. Fig. 1a illustrates the thermogravimetric profile of raw biomass of *Capparis decidua* stem. The figure indicates that decomposition of biosorbent took place in four steps. First step (30°C–300°C), corresponds to the removal of water and hemicellulose present in the biomass. The second weight loss (300°C–550°C) is matching to the

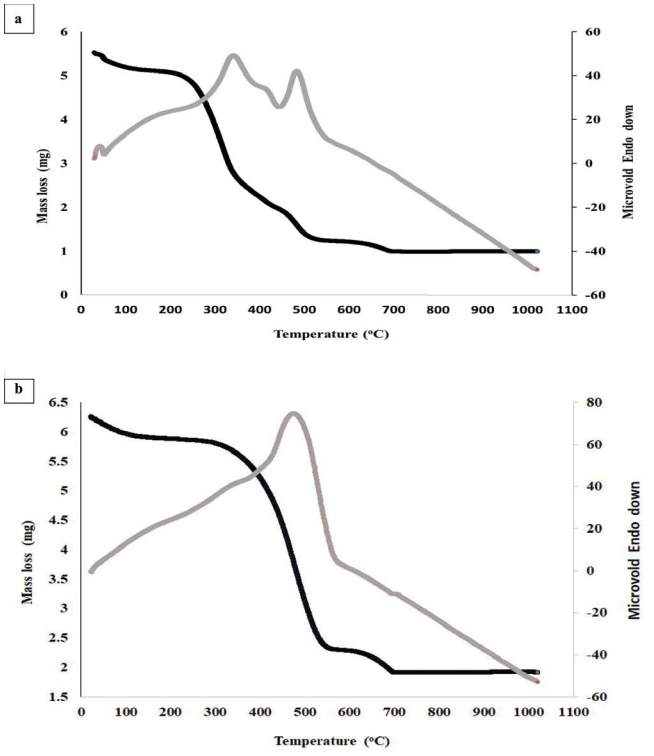

Fig. 1. Thermogravimetric analysis of (a) raw biomass and (b) activated carbon.

decomposition and thermal decomposition of different cellulose and lignin present in the stem [28]. The maximum weight loss occurred in this temperature region. In third step weight loss ranges from 550°C–700°C. This weight loss may be due to the dehydration of highly poly aromatic compounds present in the stem. Nevertheless, above 700°C, no weight loss is observed, which indicates that temperature of 700°C could be optimum temperature for preparation of activated carbon [29]. The total weight loss was 81% for biomass sample. Fig. 1b illustrates the thermogravimetric profile of ACs prepared from *Capparis decidua* stem. The decomposition of prepared activated carbon also contains three steps. The first step, occurred in temperatures range of 30°C–300°C. This weight loss is due to the removal of moisture adsorbed in micropores.It indicates a high hydrophilicity of the surfaces of activated carbon. In the second step, weight loss ranged from 300°C to 550°C. This weight loss corresponds to the decomposition of the different lignin compounds present in the stem. This indicates partial gasification of the least thermally stable fragments of carbon structure. Third step ranging from 550°C to 700°C is due to the poly aromatization by the removal of water and hydrogen from the biochar formed in 2nd stage. Heating of the sample above 700°C brought no change in the weight loss. The total weight loss up to 700°C from the sample was 68%. These results suggest that thermal treatment of the sample above 700°C could be best for preparing of the activated carbon.

FTIR technique was used for the elucidation of the different moieties which are present on the surface of raw

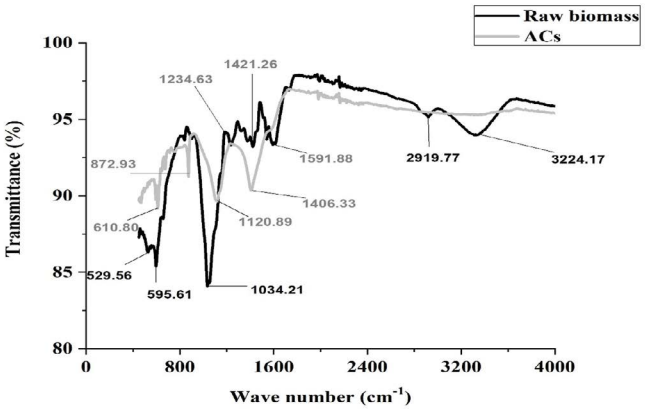

Fig. 2. FTIR analysis of (a) raw biomass and (b) activated carbon.

biomass obtained from *Capparis decidua* stem and ACs. The analysis was performed between 400 and 4,000 cm^{-1} wave number as given in Fig. 2. The figure shows that the FTIR spectrum of biomass has many functional groups like hydroxyl groups, various unsaturated hydrocarbons and carbonyl compounds. Whereas in Fig. 2b the spectrum of the prepared ACs is very simple, containing few peaks in finger print region only. As the stem of *Capparis decidua* contains two major compounds, that is, *n*-Triancontanol and Stachydrine [30]. So, the peaks may arise due to the presence of these compounds. In biomass a broad band observed at 3,324 cm^{-1}. This peak is matching the hydroxyl moiety in the literature [31]. The sharp peak observed at 2,919.77 cm^{-1} is due to the stretching of methylene C–H bond. The band observed at 1,591.88 cm^{-1} correspond to the presences of COO asymmetric stretching [32]. The peak found at 1,421.26 cm^{-1} is due to methylene C–H bending. Peaks between 1,234.63 and 1,034.21 cm^{-1} are due to the C–O bond stretching of the carbonyl or the alcohol C–O–H group. Peaks detected at 595.56 and 529.56 cm^{-1} are due to C–H deformations. In case of ACs, some functional moieties disappeared due to thermal treatment as shown in Fig. 2b. The figure shows that peak above 3,200 cm^{-1} which correspond to a hydroxyl group, disappeared due to the loss of moisture. The peak observed on 1,406.89 cm^{-1} is finger prints for the C–H bending. The peak on 1,120.89 cm^{-1} in raw biomass and at 1,030 cm^{-1} in AC represents C–O stretching vibration of stretching of alcohol and carboxylic [33,34]. Peak noted at 872.93 cm^{-1} is due to the C–C linkage of alkanes after the loss of other functionalities. Peaks observed between the 610.80–592.79 cm^{-1} are a clue to C–H deformations.

SEM technique was carried out to evaluate the topography of the raw biomass and ACs synthesized from it (Fig. 3). The figure shows that changes in the morphology of the materials in terms of size and the formation of pores were observed. It is worth noting that the pyrolysis process has altered the morphology of ACs sample compared to the raw biomass of *Capparis decidua* stem. The surface of raw biomass was rough and irregular. However, the SEM image shows that ACs have several porous. It indicates that pyrolysis method produced different types of pores and cavities on the surface. In contrast to a previous study where different activating agents were used for preparation

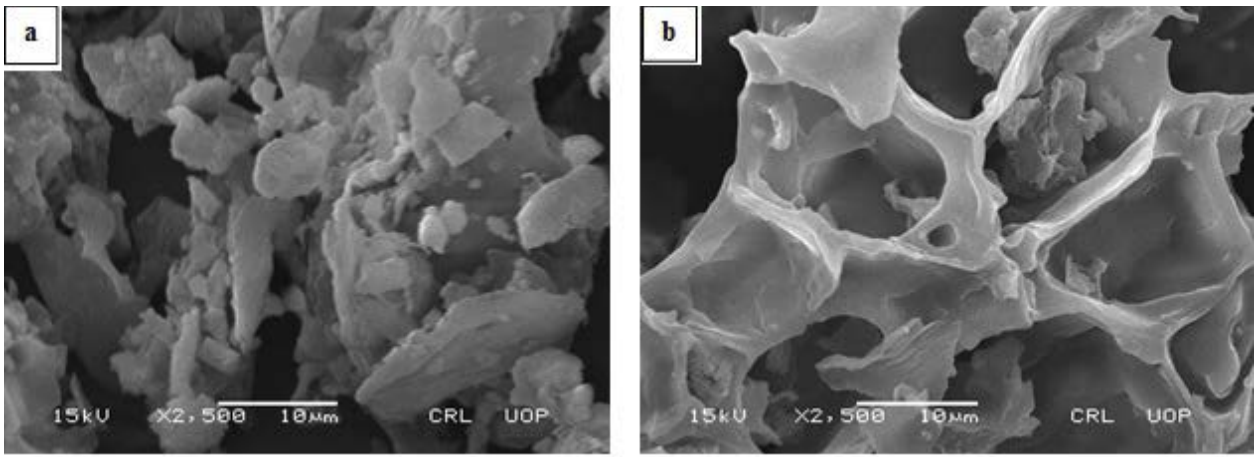

Fig. 3. SEM images of (a) raw biomass and (b) activated carbon.

of ACs, in the current results, only the thermal treatment produced pores on the surface of ACs [34]. These pores are produced due to decomposition of high H/C ratio hydrocarbons (VOC), leaving polyaromatic residue in the sample.

Chemical composition of the raw biomass and ACs prepared from *Capparis decidua* stem were analysed by energy-dispersive X-ray spectroscopy (EDX) which are shown in Table 1. From the results it was found that raw biomass contains mainly C, N and O. While ACs composed of C and O. The table indicates that the amount of carbon and oxygen contents, in raw biomass, were 48.04%, and 39.87, respectively. On the other hand, in the ACs carbon amount by weight increased to 69.99% while the oxygen amount decreased to 23.39%. A significant change between the amount of carbon/oxygen ratio in the raw and ACs samples were observed. These results indicate that synthesis of ACs from raw biomass through heat treatment brings a significant alteration in the chemical composition of ACs, which is also supported by the TGA and SEM results. The adsorbent with high carbon content has high surface area and may consider an efficient adsorbent for removal of heavy metals from waste water [35].

Table 1
EDX/EDS analysis for (a) raw biomass and (b) activated carbon

Elements	Biomass		Activated carbon	
	Weight %	Atomic %	Weight %	Atomic %
C K	48.04	55.42	69.99	77.93
N K	8.85	8.75	0.00	0.00
O K	39.87	34.35	23.39	19.55
Mg K	0.33	0.19	0.75	0.41
Si K	0.10	0.05	0.19	0.09
S K	0.94	0.41	1.23	0.51
K K	0.56	0.20	1.34	0.46
Ca K	1.32	0.46	3.11	1.04
Total		100.00		

3.2. Batch adsorption experiment

The study of various adsorption parameters such as contact time, Pb(II) concentration, dosage, rpm, pH, temperature and adsorbent particle size was examined for Pb(II) adsorption on ACs prepared from *Capparis decidua* stem and compared with raw biomass and literature.

To check the influence of concentration of Pb(II) on raw biomass and ACs, the batch analysis were performed by varying the metal concentration between 1 mg/L and 1000 mg/L while keeping other parameters such as agitation speed (140 rpm), adsorbent amount (0.1 g), temperature (25°C) and time (60 min) constant (Fig. 4). Due to the porous structure more adsorption of Pb(II) (224 mg/g) on ACs was more compared to the raw biomass (175 mg/g). It is clearly shown in the figure that adsorption increased as the concentration of Pb(II) ion increased. Equilibrium was achieved for both the adsorbents at 500 mg/L. These results indicate that at equilibrium position all the vacant sites were occupied. After filling the active sites on the adsorbent, further increase in Pb(II) concentration has no apparent change in the adsorption of Pb(II). The optimum amount of Pb(II) adsorption on ACs was compared with the previous literature (Table 2). These results explain that the prepared ACs has more Pb(II) adsorption capacity compared to the most of the biosorbent except lignin base carbon [43]. From these results, it can be concluded that prepared ACs have potential to be used as a biosorbent for removal of heavy metal from contaminated water. This high adsorption capability of the prepared ACs for Pb(II) may be due to the porous structure of the ACs which is supported by SEM analysis (Fig. 3). The high adsorption of Pb(II) on ACs can be explained by interaction of Pb(II) with oxygen containing groups (OH and COOH) which are present on the surface of ACs. It was found that functional groups present on ACs which are responsible for OH and COOH disappeared in the post reaction characterization of ACs (Fig. 5). The Pb(II) in solution make a bond with oxygen atom which is reported in previous studies [44,45].

$$2\text{R-COOH} + \text{Pb(II)} \rightarrow \text{R-COOPb(II)} + 2\text{H}^{+} \quad (12)$$

$$2\text{R-OH} + \text{Pb(II)} \rightarrow \text{R-OPb(II)} + 2\text{H}^{+} \quad (13)$$

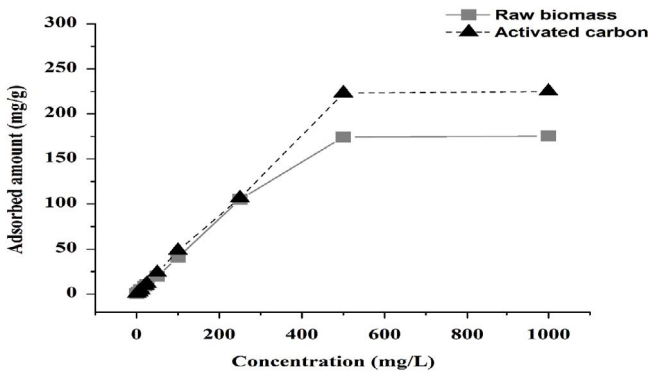

Fig. 4. Effect initial metal ion concentration on the adsorption of Pb(II) at 25°C.

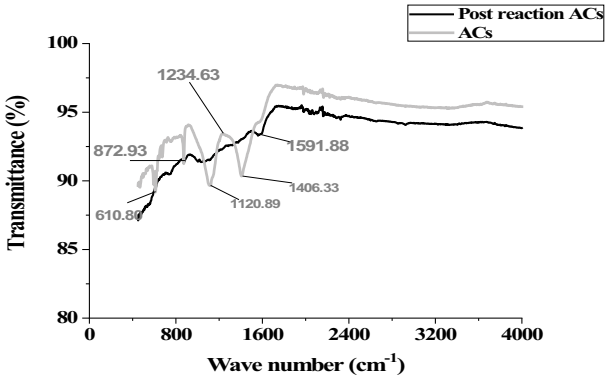

Fig. 5. Post adsorption FTIR spectrum of ACs.

Table 2
Various bioadsorbents and their adsorption capacities (mg/g) for Pb(II)

Bioadsorbent	q_{max} (mg/g)	References
Spirogyra neglecta	132.00	[36]
Cladophora fascicularis	198.5	[37]
Coconut shell	76.66	[38]
Pyrolusite-modified sewage sludge carbon	69.87	[39]
Oryza sativa L. husk	8.60	[40]
Polypyrrole-based ACs	5.54	[41]
Tea waste	1.35	[42]
Lignin-based porous carbon	250.47	[43]
Capparis decidua stem	719.42	Present work

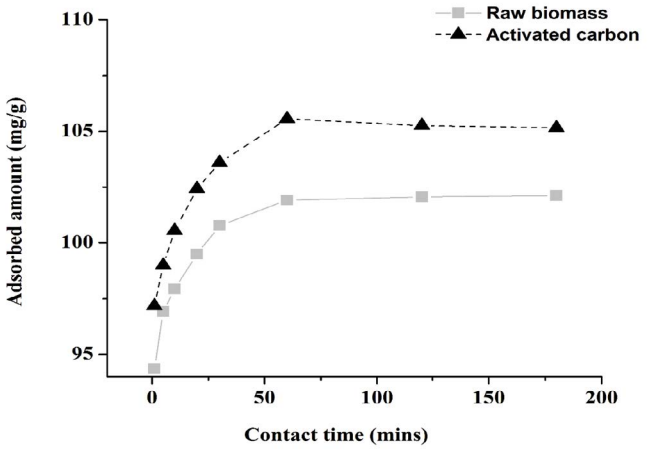

Fig. 6. Effect of contact time on the adsorption of Pb(II) on raw biomass and ACs at 25°C.

To determine the influence of contact time on both the adsorbents, adsorption of Pb(II) was performed for different interval of time which range from 1 to 180 min. Meanwhile other parameters were kept constant (Fig. 6). It was observed that initially with an increase of agitation interval, the amount of adsorption increased on biomass and ACs. However, after 60 min further increase in agitation interval brought no change in the amount of Pb(II) adsorption by the adsorbent, indicating an equilibrium has been achieved. These results show that 60 min is enough time for occupying the active sites present on both the adsorbents surface. The figure also indicates that in both the adsorbents the equilibrium was achieved in similar time (60 min) [46]. However, more Pb(II) was adsorbed on ACs than biomass. These results further supports that the vacant sites and surface area of the ACs were increased by thermal treatment. This result matches to other researches done for removal of Pb(II) on different biosorbents [47,48].

Biosorption capacity of biomass and ACs were checked by altering the dosage of adsorbent between 0.1 and 0.6 g while keeping the other parameter such as agitation speed (140 rpm) metal ion concentration (250 mg/L), the volume of sample (50 mL), temperature (25°C) and pH (6 ± 0.31) constant (Fig. 7). Maximum adsorption (121 mg/L) was observed on 0.1 g dosage of ACs. However, with an increased

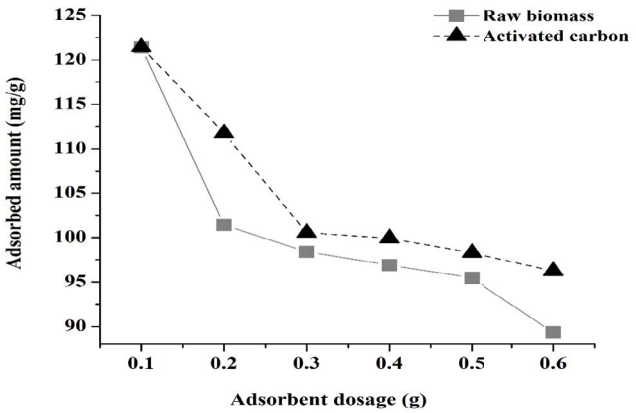

Fig. 7. Effect of biosorbent dosage on the adsorption of Pb(II).

in dosage significantly decrease the adsorption capacity of the adsorbents. This can be explained as increasing biosorbents dosage cause to overlapped or an aggregate of active sites at higher dosage and decreased in the total sorbent surface area of the biosorbent. This result is also matching with the previous literature [43,49]. In another investigation

the Pb(II) adsorption was checked on banana stalk and was found that maximum adsorption (15.8 mg/g) was taking place on 0.6 g dosage [25].

pH of solution plays a key role in governing the metal adsorption on biomass. Different optimum pH for the different nature of the biomass has been reported [15,50]. The influence of pH solution on the adsorption of Pb(II) on biomass was checked by varying the initial pH of solution between 2 and 12 at 25°C (Fig. 8). The figure indicates that adsorption of Pb(II) on the adsorbents significantly change with pH. At pH 2, the adsorption efficiency of biomass and activated carbon was low (82.2 mg/g and 86.4 mg/g). However, with an increase in pH the adsorption efficiency of both the adsorbents was increased till pH 10 and then become constant. Similar patterns of Pb(II) adsorption were observed on soybean oil cake in previous study [51]. It is proposed that there is competition between Pb(II) and H^+ for the active sites at low pH. However, at high pH the H^+ concentration is decreased and hence the Pb(II) adsorption is increased.

$$\text{At low pH:} \quad H^+ + \text{Pb(II)} + \text{☼} \rightarrow H^+ - \text{☼} + \text{Pb(II)} \quad (14)$$

$$\text{At high pH:} \quad H^+ + \text{Pb(II)} + \text{☼} \rightarrow \text{Pb(II)} - \text{☼} + H^+ \quad (15)$$

where ☼ represent active sites. These results indicate that Pb(II) adsorption onto the raw biomass and ACs is controlled by the physicochemical properties of the solution. The effect of pH study indicates that adsorption of Pb(II) followed by ion exchange path on adsorbent. At low pH the less adsorption of Pb(II) may be due to high concentration of H^+ ion in solution and on the surface of adsorbent while at high pH decrease of H^+ and increase of negative charge on the surface increased the adsorption efficiency of Pb(II) on the surface which is supported by the point of zero charge (PZC). The figure also indicates that after pH 8 the removal efficiency significantly increased [52].

The change of adsorption temperature influence the equilibrium sorption capacity for both the chemisorption and physiosorption process [53]. In this study, temperature was varied between 5°C and 70°C while the other parameters remain constant as given in Fig. 9. The results showed that increase of temperature from 5°C to 40°C give almost similar patterns for both the adsorbents. After 40°C, further increase in temperature significantly decreased the rate of adsorption which steadily decreased till to 70°C. These results reveal that adsorption of Pb(II) on raw biomass and ACs is function on temperature and increase of the temperature decrease the adsorption process, similar result are also reported in literature [54]. From these results, it is concluded that adsorption of Pb(II) is physiosorption. The current results show that Pb(II) on biomass is exothermic in nature. Therefore, in accordance with Le-Chatelier's principle, with an increase in temperature adsorption of Pb(II) on adsorbent decreased, which support that physiosorption occurred more easily at a lower temperature. This result indicates that at room temperature the use of this ACs has potential to be used for removal of Pb(II) from contaminated water.

The size of particle influence on the active sites and diffusion of the metal ion inside the structure of the particle [55]. The effect of adsorbent particle size was investigated from 45 to 250 μm using 50 mL of solution with metal ion concentration of 250 mg/L at 25°C as given in Fig. 10. The figure shows that with an increase of particle size from 45 to 250 μm the removal of Pb(II) decreased from 121 to 109 mg/g. This result indicates that efficiency of small particle for removal of metal ions is higher than

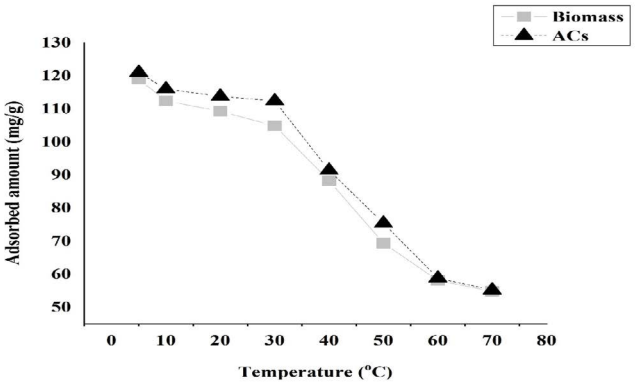

Fig. 9. Effect of temperature on adsorption of Pb(II) on raw biomass and ACs.

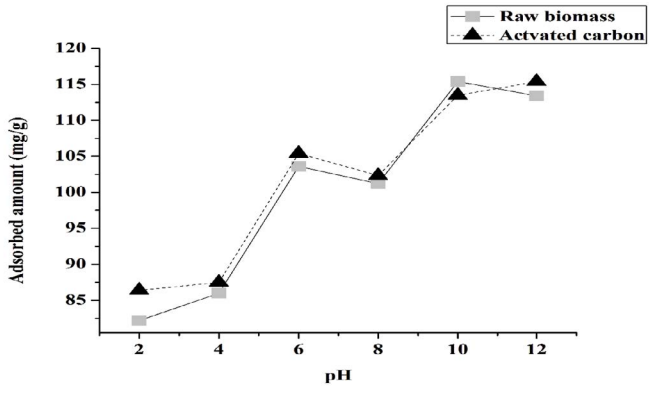

Fig. 8. Effect of pH on Pb(II) adsorption at 25°C.

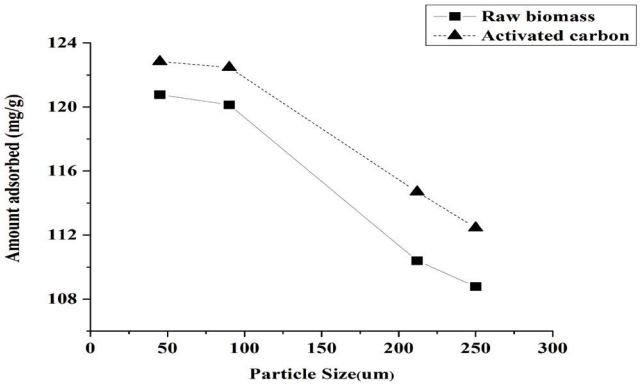

Fig. 10. Effect of adsorbent particle size on Pb(II) adsorption at 25°C.

large particle size. This clues that an increase of the particle decreases the surface area and hence decreases the Pb(II) adsorption on the ACs and raw biomass [55].

PZC illustrates about the presence of positive and negative charge carrying functional moieties on the surface of the adsorbent. The amphoteric nature of carbon may have a positive or negative charge, depending upon the surface functional moieties and the pH of the solution. Below PZC the surface favors the adsorption of negative charge while pH above PZC favor positive charge species [51]. pH at PZC was determined for the raw biomass and ACs which is illustrated in Fig. 11. The figure elaborates that pH at PZC were 7.5 and 8.8 for raw biomass and ACs respectively. These results indicate that thermal treatment modify the number and nature of surface functional groups and give a different pH at PZC.

3.3. Adsorption kinetics

For the commercialization of adsorbent, kinetics study is important for adsorption. The nature and type of the adsorption method is a function of the chemical and physical behaviors of adsorbent and the other parameter of the system. For the adsorption kinetic study, pseudo-first-order and pseudo-second-order kinetics models were applied. The integrated form of pseudo-first-order kinetics model [Eq. (3)] was applied on the obtained results. The current results indicate that first order kinetics model does not apply to our system due to low correlation coefficient value (R^2) of 0.60938 for biomass and 0.80762 for ACs (Table 3). Biosorption of Pb(II) on *Anethum graveolens* is also matches with the current results [56]. High linearity of correlation coefficient value (R^2) was observed in case of pseudo-second-order kinetic model [Eq. (4)]. Also, adsorption capacity (q_e) was close to the experimental value (Fig. 12). k_2, q_e, and R^2 values calculated from the graph are tabulated in Table 3. So, it can be concluded that pseudo-second-order kinetic model is well fitted to our kinetic results of Pb(II) adsorption on raw biomass and ACs prepared form *Capparis decidua*. These results have close agreement with the previous literature [57,58]. pseudo-second-order kinetic equation is also followed by adsorption of Pb(II) on the orange peel, peanut shell and tea waste [59].

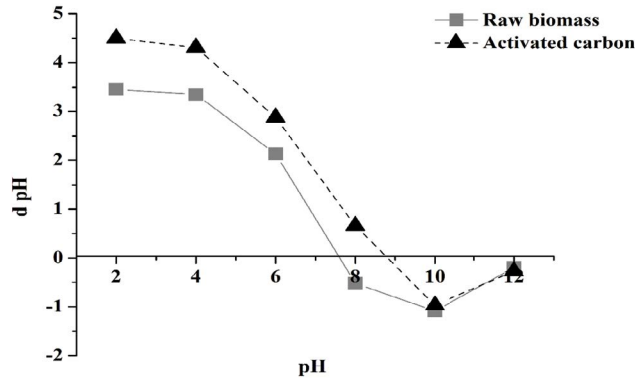

Fig. 11. pH at PZC for raw biomass and activated carbon.

Weber and Morris model is used to determine the rate-limiting step of the movement of metals from solution on the surface and inside the particle. To determine, whether Pb(II) diffusion on raw biomass and ACs is intra-particle diffusion control or boundary layer diffusion control, an amount of adsorbed Pb(II) was plotted verses the square root of the time using Morris equation.

$$q_1 = k_1 t^{1/2} + C \tag{16}$$

where q_t represents the amount of Pb(II) adsorbed at a particular time, K_i is rate constant for the intra-particle diffusion and C represent the intercept of the graph (Fig. 13) [60]. The figure shows that adsorption of Pb(II) on adsorbent completed in two steps. In the first step the adsorption of Pb(II) sharply increased up to 6 min. This change in the adsorption of Pb(II) in the initial 6 min may correlate to the diffusion of adsorbate from the solution to the external surface of the adsorbent or the boundary layer diffusion of the biosorbate molecules. In the 2nd the step no

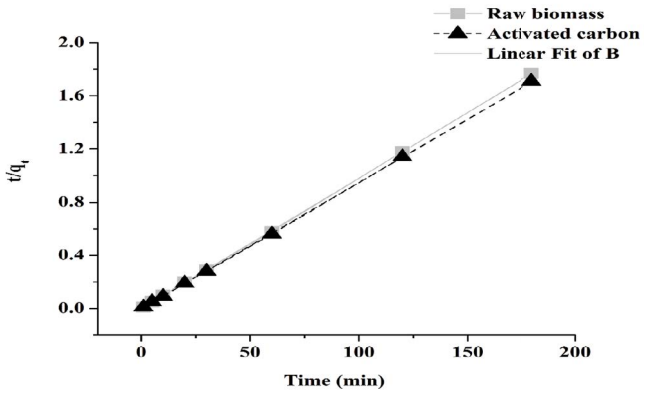

Fig. 12. Pseudo-second-order kinetic for the adsorption of Pb(II) on raw biomass and ACs.

Table 3
Pseudo-first-order and pseudo-second-order results

Kinetic models	Constants	Adsorbents	
		Biomass	Activated carbon
Pseudo-first-order model			
	R^2	0.6094	0.8076
	k_1 (1/s)	0.0129	–0.0178
	q_e (mg/g) (experimental)	101.921	5.55
	q_e (mg/g) (calculated)	1.288	1.6120
Pseudo-second-order model			
	R^2	0.9999	0.9999
	k_2 (M/s)	0.044	0.042
	q_e (mg/g) (experimental)	101.92	105.55
	q_e (mg/g) (calculated)	101.72	105.26
	$1/k_2 q_e^2$	0.0022	0.00211

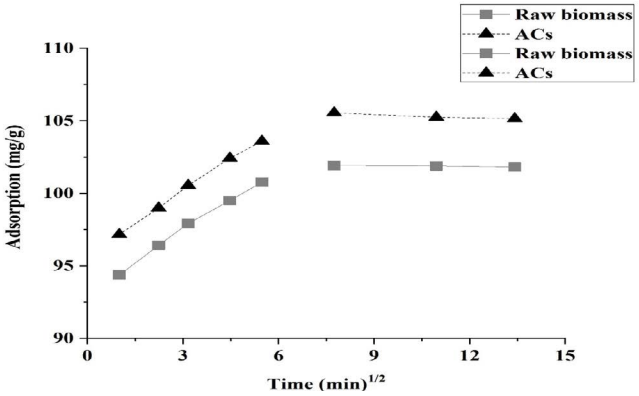

Fig. 13. Morris and Weber linear plot for Pb(II) adsorption on (a) raw biomass and (b) activated carbon.

Table 4
Constants of Freundlich and Langmuir isotherm model

		Adsorbents	
Isotherm models	Constants	Biomass	Activated carbon
Freundlich			
	R^2	0.9149	0.9910
	K_f (mg/g)	0.75763	0.7106
	$1/n$	0.91489	0.9763
Langmuir			
	R^2	0.8387	0.5834
	K_L (dm^3/L)	0.0013	0.0006
	R_L	0.615	0.757
	q_m (mg/g)	327.86	719.42

apparent change in the adsorption of (Pb(II) was detected, which indicates that the equilibrium position of adsorbate was achieved after 6 min. The extrapolation of the data does not pass through the origin. These results deduced that adsorption of Pb(II) is not intraparticle diffusion control, but it likes to be boundary layer control [61].

3.4. Adsorption isotherms

At fixed temperature, the adsorbent and adsorbate interaction and the degree of adsorption on the surface of an adsorbent can be evaluated by adsorption model. Adsorbent surface may be monolayer or multilayer depending upon the model which are followed by the data. Among different isotherms, Langmuir, Freundlich and Morris model are studied and compared [62].

Monolayer adsorption of Pb(II) from a liquid solution on a surface of raw biomass and ACs can be well explained by Langmuir model. This model gives an idea about vacant sites which have a fixed number of vacant sites. The isotherm data is presented in Table 4. Langmuir isotherm model was not applicable to our data due to low correlation coefficient value (R^2) of 0.83874 for biomass and 0.5834 for ACs. A Freundlich isotherm model is used to explain multilayer adsorption of adsorbed molecules on a heterogeneous surface which have non uniform distribution of heat of adsorption. From Table 4 it can be seen that the K_f value of biomass (0.757 mg/g) is greater than ACs (0.710 mg/g). Freundlich isotherm model is well matched with the results due to high correlation coefficients value (0.990). This result has close agreement with previous literature, where Pb(II) adsorption on marine green algae follows Freundlich model [47]. The adsorption intensity value ($1/n$) for biomass and activated carbon are >0.05, indicates that the interaction between adsorbate and adsorbent during the adsorption process is feasible.

3.5. Thermodynamics analysis for Pb(II) adsorption

The thermodynamics feasibility of Pb(II) adsorption on biomass and ACs was calculated using different parameters such as enthalpy, entropy and change in Gibbs free energy (Tables 5 and 6). The determination of $\Delta G°$ is the criteria for spontaneity of physiochemical process. For calculation of Gibbs free energy we need to calculate the equilibrium constant. The equilibrium constant K_0 value was determined at different temperatures as given in section 2.8. The change in enthalpy ($\Delta H°$) was evaluated by van't Hoff equation:

$$\ln K_0\left(T_2\right) - \ln K_0\left(T_1\right) = \frac{-\Delta H°}{R}\left(\frac{1}{T_2} - \frac{1}{T_1}\right) \tag{17}$$

T_2 and T_1 represents final and initial temperatures.

The higher value of equilibrium constant on ACs compared to biomass indicates that more adsorption took place on ACs. From the tables it was found that at low temperature the change in Gibbs free energy was high which decreased with an increase of temperature. These results elaborate that process of Pb(II) adsorption decreased on both biomass and ACs adsorbent with an increase of temperature and hence conclude that Pb(II)adsorption on both the adsorbents is physiosorption in nature [6]. Also higher negative value of $\Delta G°$ support more adsorption on ACs compared to biomass while at higher temperature biomass and ACs have similar adsorption. These results further support that adsorption on both the adsorbents are physiosorption in nature. The negative value of enthalpy clues that lead adsorption on both the adsorbents are exothermic in nature [63].

4. Conclusions

In this study, the effective use of the ACs prepared from *Capparis decidua* stem as an adsorbent for removing of Pb(II) from model aqueous solution was investigated. For synthesis of ACs from the stem of *Capparis decidua*, optimum activation temperature was found from 500°C to 700°C. Thermal treatment brings a significant change in the morphology and chemical composition of ACs. At equilibrium, the highest adsorption of Pb(II) was found 224 mg/g and the equilibrium position was achieved with in the initial 60 min. It was found from the batch experiment that experimental results follow the pseudo-second-order and are well fitted in the Freundlich isotherm

Table 5
Thermodynamic parameters ($\Delta G°$, $\Delta H°$, $\Delta S°$) results for raw biomass

Thermodynamic constants	Temp. (K)							
	278	283	293	303	313	323	333	343
K_0 (mL $g^{-1)}$	6,444.44	4,460.31	3,480.89	2,609.45	1,202.99	624.10	434.23	390.31
$\Delta G°$ (kJ mol^{-1})	–20.250	–19.749	–19.832	–19.790	–18.451	–17.280	–16.778	–16.987
$\Delta H°$ (kJ mol^{-1})	–36.443							
$\Delta S°$ (J mol^{-1} K^{-1})	16.0							

Table 6
Thermodynamic parameters ($\Delta G°$, $\Delta H°$, $\Delta S°$) results for activated carbon

Thermodynamic constants	Temp. (K)							
	278	283	293	303	313	323	333	343
K_0 (mL $g^{-1)}$	16,861.	6,444.4	5,080.3	4,460.3	1,360.1	760.08	444.10	395.41
$\Delta G°$ (kJ mol^{-1})	–22.468	–20.627	–20.753	–21.129	–18.744	–17.782	–16.862	–17.029
$\Delta H°$ (kJ mol^{-1})	–45.396							
$\Delta S°$ (J mol^{-1} K^{-1})	29.70							

model. In basic media the adsorption of Pb(II) on both the adsorbents was higher and pH for PZC was found 8.8 on ACs. The $-\Delta G°$ and $-\Delta H°$ confirm that adsorption of Pb(II) is favorable and exothermic in nature on the ACs. Based on the current findings, it can be concluded that ACs prepared from *Capparis decidua* stem is considered to be a cheap, eco-friendly biosorbent which will be effective for removing of Pb(II) from wastewater.

Acknowledgments

The authors are grateful to Kohat University of Science and Technology, Kohat Khyber Pakhtunkhwa for providing Lab and instrumental facilities in completion of this project.

References

[1] G. Lamzougui, H. Nafai, D. Chafik, A. Bouhaouss, R. Bchitou, Adsorption of Lead(II) onto Phosphogypsum from liquid effluents, Der Pharma Chemica, 9 (2017) 109–113.
[2] J.L. Wang, C. Chen, Biosorbents for heavy metals removal and their future, Biotechnol. Adv., 27 (2009) 195–226.
[3] J. Cruz-Olivares, G. Martínez-Barrera, C. Pérez-Alonso, C.E. Barrera-Díaz, M. del Carmen Chaparro-Mercado, F. Ureña-Núñez, Adsorption of lead ions from aqueous solutions using gamma irradiated minerals, J. Chem., 2016 (2016) 8782469, https://doi.org/10.1155/2016/8782469.
[4] M. Bilal, J. Ali, N. Hussain, M. Umar, S. Shujah, D. Ahmad, Removal of Pb(II) from wastewater using activated carbon prepared from the seeds of *Reptonia buxifolia*, J. Serb. Chem. Soc., 85 (2020) 265–277.
[5] A. Azimi, A. Azari, M. Rezakazemi, M. Ansarpour, Removal of heavy metals from industrial wastewaters: a review, ChemBioEng Rev., 4 (2017) 37–59.
[6] M. Zbair, Z. Anfar, H. Ait Ahsaine, N. El Alem, M. Ezahri, Acridine orange adsorption by zinc oxide/almond shell activated carbon composite: operational factors, mechanism and performance optimization using central composite design and surface modelling, J. Environ. Manage., 206 (2018) 383–397.
[7] H.I. Albroomi, M.A. Elsayed, A. Baraka, M.A. Abdelmaged, Batch and fixed-bed adsorption of tartrazine azo-dye onto activated carbon prepared from apricot stones, Appl. Water Sci., 7 (2017) 2063–2074.
[8] K. Kadirvelu, M. Palanival, R. Kalpana, S. Rajeswari, Activated carbon from an agricultural by-product, for the treatment of dyeing industry wastewater, Bioresour. Technol., 74 (2000) 263–265.
[9] M. Teker, M. Imamoglu, O. Saltabas, Adsorption of copper and cadmium ions by activated carbon from rice hulls, Turk. J. Chem., 23 (1999) 185–191.
[10] M. Kaur, S. Kumari, P. Sharma, Removal of Pb(II) from aqueous solution using nanoadsorbent of *Oryza sativa* husk: isotherm, kinetic and thermodynamic studies, Biotechnol. Rep., 25 (2020) 410–416.
[11] A.M. Aljeboree, A.N. Alshirifi, A.F. Alkaim, Kinetics and equilibrium study for the adsorption of textile dyes on coconut shell activated carbon, Arabian J. Chem., 10 (2017) S3381–S3393.
[12] L.C. Morais, E.P. Gonçalves, L.T. Vasconcelos, C.G. González Beça, Reactive dyes removal from wastewaters by adsorption on eucalyptus bark – adsorption equilibria, Environ. Technol., 21 (2000) 577–583.
[13] J.C. Moreno-Piraján, L. Giraldo, Heavy metal ions adsorption from wastewater using activated carbon from orange peel, E-J. Chem., 9 (2012) 926–937.
[14] J.H. Yan, G.H. Lan, H.Y. Qiu, C. Chen, Y.Q. Liu, G.Y. Du, J.H. Zhang, Adsorption of heavy metals and methylene blue from aqueous solution with citric acid modified peach stone, Sep. Sci. Technol., 53 (2018) 1678–1688.
[15] I.U. Salihi, S.R.M. Kutty, M.H. Isa, Adsorption of lead ions onto activated carbon derived from sugarcane bagasse, IOP Conf. Ser.: Mater. Sci. Eng., 201 (2017) 012034.
[16] L.B.L. Lim, N. Priyantha, S.A.A. Latip, Y.C. Lu, A.H. Mahadi, Converting *Hylocereus undatus* (white dragon fruit) peel waste into a useful potential adsorbent for the removal of toxic Congo red dye, Desal. Water Treat., 185 (2020) 307–317.
[17] L.B.L. Lim, N. Priyantha, X.H. Bong, N.A.H.M. Zaidi, Enhancement of adsorption characteristics of Methyl violet 2B dye through NaOH treatment of *Cucumis melo var. cantalupensis* (rock melon) skin, Desal. Water Treat., 180 (2020) 336–348.

[18] L.B.L. Lim, N. Priyantha, K.J. Mek, N.A.H.M. Zaidi, Potential use of *Momordica charantia* (bitter gourd) waste as a low-cost adsorbent to remove toxic crystal violet dye, Desal. Water Treat., 82 (2017) 121–130.
[19] S. Karthikeyan, P. Sivakumar, P.N. Palanisamy, Novel activated carbons from agricultural wastes and their characterization, E-J. Chem., 5 (2008) 902073, https://doi.org/10.1155/2008/902073.
[20] E. Vunain, D. Kenneth, T. Biswick, Synthesis and characterization of low-cost activated carbon prepared from Malawian baobab fruit shells by H_3PO_4 activation for removal of Cu(II) ions: equilibrium and kinetics studies, Appl. Water Sci., 7 (2017) 4301–4319.
[21] E.N. Bakatula, D. Richard, C.M. Neculita, G.J. Zagury, Determination of point of zero charge of natural organic materials, Environ. Sci. Pollut. Res. Int., 25 (2018) 7823–7833.
[22] R. Mallampati, S. Valiyaveettil, Application of tomato peel as an efficient adsorbent for water purification alternative biotechnology, RSC Adv., 2 (2012) 9914–9920.
[23] Y.S. Ho, G. McKay, Pseudo-second-order model for sorption processes, Process Biochem., 34 (1998) 451–465.
[24] K.R. Hall, L.C. Eagleton, A. Acrivos, T. Vermeulen, Pore- and solid-diffusion kinetics in fixed-bed adsorption under constant-pattern conditions, Ind. Eng. Chem. Res., 5 (1966) 212–223.
[25] O.O. Ogunleye, A.A. Mary, S.E. Agarry, Evaluation of biosorptive capacity of banana (*Musa paradisiaca*) stalk for Lead(II) removal from aqueous solution, J. Environ. Prot. Sci., 5 (2014) 1451–1465.
[26] A.A.A. Daifullah, B.S. Girgis, H.M.H. Gad, A study of the factors affecting the removal of humic acid by activated carbon prepared from biomass material, Colloids Surf., A, 235 (2004) 1–10.
[27] S.-Y. Lin, An overview of advanced hyphenated techniques for simultaneous analysis and characterization of polymeric materials, Crit. Rev. Solid State Mater. Sci., 41 (2016) 482–530.
[28] A. Saffe, A. Fernandez, G. Mazza, Prediction of regional agro-industrial wastes characteristics by thermogravimetric analysis to obtain bioenergy using thermal process, Energy Explor. Exploit., 37 (2019) 544–557.
[29] C.I. Contescu, S.P. Adhikari, N.C. Gallego, N.D. Evans, B.E. Biss, Activated carbons derived from high-temperature pyrolysis of lignocellulosic biomass, J. Carbon Res., 4 (2018) 2–16.
[30] S. Rathee, P. Rathee, D. Rathee, D. Rathee, V. Kumar, Phytochemical and pharmacological potential of Kair (*Capparis Decidua*), Int. J. Phytomed., 2 (2010) 10–17.
[31] M. Demir, K.S. Saraswat, R.B. Gupta, Hierarchical nitrogen-doped porous carbon derived from lecithin for high-performance supercapacitors, RSC Adv., 7 (2017) 42430–42442.
[32] D. Kalaiselvi, R.M. Kumar, R. Jayavel, Single crystal growth and properties of semiorganic nonlinear optical L-arginine hydrochloride monohydrate crystals, Cryst. Res. Technol., 43 (2008) 851–856.
[33] I.H. Boyaci, H.T. Temiz, H.E. Geniş, E.A. Soykut, N.N. Yazgan, B. Güven, R.S. Uysal, A.G. Bozkurt, K. İlaslan, O. Toruna, F.C.D. Şekera, Dispersive and FT-Raman spectroscopic methods in food analysis, RSC Adv., 5 (2015) 56606–56624.
[34] İ. Demiral, C.A. Şamdan, Preparation and characterization of activated carbon from pumpkin seed shell using H_3PO_4, J. Appl. Sci. Eng., 17 (2016) 125–138.
[35] S.X. Zhao, N. Ta, X.D. Wang, Effect of temperature on the structural and physicochemical properties of biochar with apple tree branches as feedstock material, Energies, 10 (2017) 1–15.
[36] M.A. Hussain, A. Salleh, P. Milow, Characterization of the adsorption of the Lead(II) by the non-living biomass *Spirogyra neglecta* (Hasall) Kutzing, Am. J. Biochem. Biotechnol., 5 (2009) 75–83.
[37] L.P. Deng, Y.Y. Su, H. Su, X.T. Wang, X.B. Zhu, Sorption and desorption of lead(II) from wastewater by green algae *Cladophora fascicularis*, J. Hazard. Mater, 14 (2007) 220–225.
[38] K. Singh, M. Gautam, B. Chandra, A. Kumar, Removal of Pb(II) from its aqueous solution by activated carbon derived from Balam Khira (Kigelia Africana), Desal. Water Treat., 57 (2016) 24487–24497.
[39] L. Fan, Y. Chen, L. Wang, W.J. Jiang, Adsorption of Pb(II) ions from aqueous solutions by pyrolusite-modified activated carbon prepared from sewage sludge, Adsorpt. Sci. Technol., 29 (2011) 495–506.
[40] M.M.D. Zulkali, A.L. Ahmad, N.H. Norulakmal, *Oryza sativa* L. husk as heavy metal adsorbent: optimization with lead as model solution, Bioresour. Technol., 97 (2006) 21–25.
[41] A.A. Alghamdi, A.-B. Al-Odayni, W.S. Saeed, A. Al-Kahtani, F.A. Alharthi, T. Aouak, Efficient adsorption of Lead(II) from aqueous phase solutions using polypyrrole-based activated carbon, Materials (Basel), 12 (2019) 2020–2035.
[42] M.K. Mondal, Removal of Pb(II) from aqueous solution by adsorption using activated tea waste, Korean J. Chem. Eng., 27 (2010) 144–151.
[43] A.Q. Wang, Z.K. Zheng, R.Q. Li, D. Hu, Y.R. Lu, H.X. Luo, K. Yan, Biomass-derived porous carbon highly efficient for removal of Pb(II) and Cd(II), Green Energy Environ., 4 (2019) 414–423.
[44] R. Xie, Y. Jin, Y. Chen, W. Jiang, The importance of surface functional groups in the adsorption of copper onto walnut shell derived activated carbon, Water Sci Technol., 76 (2017) 3022–3034.
[45] A. Kuroki, M. Hiroto, Y. Urushihara, T. Horikawa, K. Sotowa, J.R.A. Avila, Adsorption mechanism of metal ions on activated carbon, Adsorption, 25 (2019) 1251–1258.
[46] G. Wang, S. Zhang, P. Yao, Y. Chen, X. Xu, T. Li, G. Gong, Removal of Pb(II) from aqueous solutions by *Phytolacca americana* L. biomass as a low cost biosorbent, Arabian J. Chem., 11 (2018) 99–110.
[47] R.P.S. Jeyakumar, V. Chandrasekaran, Adsorption of lead(II) ions by activated carbons prepared from marine green algae: equilibrium and kinetics studies, Int. J. Ind. Chem., 5 (2014) 1–9.
[48] G.A. Adebisi, Z.Z. Chowdhury, P.A. Alaba, Equilibrium, kinetic, and thermodynamic studies of lead ion and zinc ion adsorption from aqueous solution onto activated carbon prepared from palm oil mill effluent, J. Cleaner Prod., 148 (2017) 958–968.
[49] H.Z. Mousavi, A. Hosseynifar, V. Jahed, S.A.M. Dehghani, Removal of Lead from aqueous solution using waste tire rubber ash as an adsorbent, Braz. J. Chem. Eng., 27 (2010) 79–87.
[50] R.B. Shaikh, B. Saifullah, F. Rehman, Greener method for the removal of toxic metal ions from the wastewater by application of agricultural waste as an adsorbent, Water, 10 (2018) 3018–3029.
[51] M. Erdem, S. Ucar, S. Karagöz, T. Tay, Removal of lead(II) ions from aqueous solutions onto activated carbon derived from waste biomass, Sci. World J., 2013 (2013) 1–7.
[52] H. Karimi, Effect of pH and initial Pb(II) concentration on the lead removal efficiency from industrial wastewater using $Ca(OH)_2$, Int. J. Water Wastewater Treat., 3 (2017) 1–4.
[53] H.I. Adegoke, F.A. Adekola, I.T. Olowookere, A.L. Yaqub, Thermodynamic studies on adsorption of Lead(II) ion from aqueous solution using magnetite, activated carbon and composites, J. Appl. Sci. Environ. Manage., 21 (2017) 440–452.
[54] S.S. Majumdar, S.K. Das, R. Chakravarty, T. Saha, T.S. Bandyopadhyay, A.K. Guha, A study on lead adsorption by *Mucor rouxii* biomass, Desalination, 251 (2010) 96–102.
[55] H.N. Bhatti, A. Saleem, M.A. Hanif, Utilization of *Mentha arvensis* waste biomass for the removal of Pb(II) and Co(II) from aqueous solutions, Desal. Water Treat., 51 (2013) 3335–3343.
[56] A. Hashem, K. El-Khiraigy, Bioadsorption of Pb(II) onto *Anethum graveolens* from contaminated wastewater: equilibrium and kinetic studies, J. Environ. Prot. Sci., 4 (2013) 108–119.
[57] J. Shah, M.R. Jan, M. Khan, S. Amir, Removal and recovery of cadmium from aqueous solutions using magnetic nanoparticle-modified sawdust: kinetics and adsorption isotherm studies, Desal. Water Treat., 57 (2016) 9736–9744.
[58] A.E. Ofomaja, Biosorption studies of Cu(II) onto Mansonia sawdust: process design to minimize biosorbent dose and contact time, React. Funct. Polym., 70 (2010) 879–889.
[59] S. Yorgun, D. Yıldız, Preparation and characterization of activated carbons from Paulownia wood by chemical activation with H_3PO_4, J. Taiwan Inst. Chem. Eng., 53 (2015) 122–131.

[60] I. Tsibranska, E. Hristova, Comparison of different kinetic models for adsorption of heavy metals onto activated carbon from apricot stones, Bulg. Chem. Commun., 43 (2011) 370–377.
[61] A.E. Ofomaja, Intraparticle diffusion process for lead(II) biosorption onto Mansonia wood sawdust, Bioresour. Technol., 101 (2010b) 5868–5876.
[62] M.T. Amin, A.A. Alazba, M. Shafiq, Adsorptive removal of reactive black 5 from wastewater using bentonite clay: isotherms, kinetics and thermodynamics, Sustainability, 7 (2015) 15302–15318.
[63] L. Largitte, P. Lodewyckx, Kinetics and thermodynamics of the adsorption of lead(II) on a activated carbon from coconut shells, Eurasian Chem. Technol. J., 15 (2013) 283–292 and 82 (2017) 121–130.